ELSEVIER

Journal of Magnetism and Magnetic Materials 195 (1999) 327–335

Journal of magnetism and magnetic materials

Spin configurations and magnetization reversal processes in ultrathin cubic ferromagnetic films with in-plane uniaxial anisotropy

Ming-hui Yu*, Zhi-dong Zhang, Tong Zhao

Institute of Metal Research, Chinese Academy of Sciences, 72 Wenhua Road, Shenyang 110015, People's Republic of China and International Center for Materials Physics, Chinese Academy of Sciences, Shenyang 110015, People's Republic of China

Received 8 October 1998; received in revised form 11 January 1999

Abstract

Based on a phenomenological model, spin structures either in the absence or in the presence of an external magnetic field have been studied for ultrathin cubic ferromagnetic films with an in-plane uniaxial anisotropy. Phase diagrams of the spin configurations in the absence of the magnetic field and of different magnetization reversal processes have been given. The magnetization reversal processes in the ultrathin cubic ferromagnetic films have been found to depend sensitively on the competition among the energies of in-plane uniaxial and cubic anisotropies and of the domain wall pinning.

PACS: 75.60. − d; 75.70. − i; 75.25. + z

Keywords: Ultrathin films; Spin configuration; In-plane uniaxial anisotropy; Magnetization reversal process; Domain wall pinning

1. Introduction

In recent years, ultrathin ferromagnetic films have attracted a tremendous amount of attention. Magnetic anisotropies play an important role in ultrathin ferromagnetic films. Anisotropy is necessary in two-dimensional ferromagnets to obtain long-range order, as proven rigorously by Mermin and Wagner [1]. Magnetic anisotropies in ultrathin films are strongly modified, compared to those in bulk materials, due to the broken symmetry at the interface. These anisotropies include shape, surface, interface, and crystalline anisotropies, strain-induced magnetoelastic anisotropy, and anisotropies due to roughness, steps and atomic mixing at the interface [2].

One of the most fascinating topics in this field is how to understand the unusual magnetization reversal processes which take place in some ultrathin cubic ferromagnetic films [3–12]. In these processes the in-plane spin configuration changes abruptly at

* Correspondence author. Tel.: + 86-24-2384-3531-55857; fax: + 86-24-2389-1320.

E-mail address: dygeng@imr.ac.cn (M. Yu)

0304-8853/99/$ – see front matter
PII: S0304-8853(99)00139-0

well-defined strengths and orientations of an applied magnetic field, which is unexpected for ultrathin films with purely cubic magnetocrystalline anisotropy. These peculiar magnetic switching processes were attributed to the occurrence of a weak in-plane uniaxial anisotropy which was superimposed on the strong cubic magnetocrystalline anisotropy. Cowburn et al. [13,14] recently developed a simple phenomenological model, explaining how so small a uniaxial anisotropy can significantly influence the magnetization reversal processes. In their model a well-defined domain wall (DW) pinning energy is considered along with the anisotropy energy surface in order to determine the energetics of the reversal processes. A good agreement has been established between the model prediction and the experimental observation [10–14]. However, Cowburn et al. [13,14] focused their attention only on the behaviors of Fe ultrathin films, i.e., the case of a positive in-plane uniaxial anisotropy. In the present work, we extend their discussion to the whole system, including the situation with a negative in-plane cubic anisotropy which indeed corresponds to Co ultrathin films [15–18].

2. Model

The phenomenological model to be studied in what follows is defined by the free energy [13,14]

$$E(\theta) = K_u \sin^2\theta + K_1 \sin^2\theta \cos^2\theta - MH\cos(\theta - \phi), \quad (1)$$

where K_u is the in-plane uniaxial anisotropy constant, K_1 is the in-plane cubic anisotropy constant, θ and ϕ are the angles of the magnetization M and the applied field H with respect to the a-axis [1 0 0] direction, respectively, as shown in Fig. 1. The equilibrium state is found by minimizing Eq. (1) with respect to the angle θ. This involves the first and second partial derivatives of the free energy with respect to the angle θ,

$$\frac{\partial E}{\partial \theta} = K_u \sin 2\theta + K_1 \sin 2\theta \cos 2\theta + MH\sin(\theta - \phi) = 0, \quad (2)$$

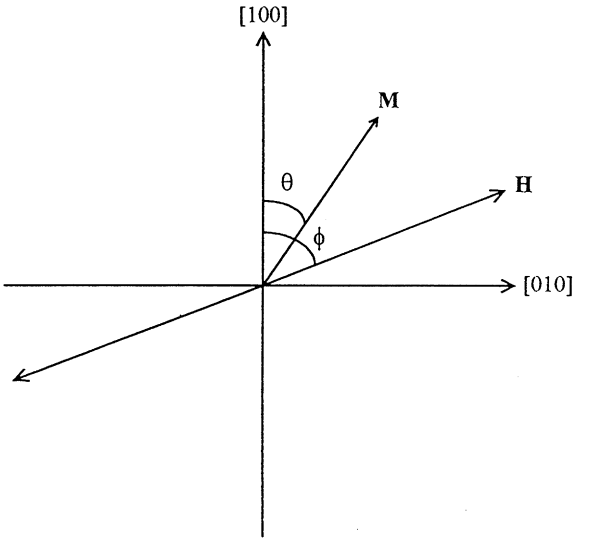

Fig. 1. Schematic representation of the geometry of spin moment M and applied magnetic field H in the plane of an ultrathin film.

$$\frac{\partial^2 E}{\partial \theta^2} = 2K_u \cos 2\theta + 2K_1 \cos 4\theta + MH\cos(\theta - \phi) > 0. \quad (3)$$

The solutions satisfying Eqs. (2) and (3) correspond to the local energy minima. There is a problem how to choose the resulting spin orientation among these solutions, if they are not sole. Departing from the Stoner–Wohlfarth's coherent rotation model [19], one can take the resulting spin orientation always corresponding to the configuration of absolute energy minimum which is determined by choosing between all the local energy minima calculated for a given set of parameters [20]. Magnetization curves calculated in this case never show hysteresis, as the energy wall between the different local minima is neglected during the spin reversal process. In real materials, however, the magnetization reversal process also involves the nucleation of domains and the propagation of domain walls [4,5,21,22]. Therefore, the energetics of domain formation and propagation are crucial in understanding the spin reversal process. Following the method developed in Refs. [13,14], a phenomenological constant ε is taken into account, which

describes the pinning energy of a DW, and corresponds to the maximum pinning pressure that defects can exert on a DW as it propagates. Before the spin transition from one local energy minimum to another lower one, the energy advantage ΔE between these two minima must be equal to the energy cost in propagating a DW of the relevant type. The activation energy needed to establish these walls is ignored, and we take care of only the drive energy involved in unpinning them so that they can sweep freely across the film. Setting $\varepsilon = 0$ for any type of DW, we will return to the former case, i.e., comparing the absolute energy minimum directly.

3. Spin configurations at $H = 0$

In this section, we shall discuss the spin configurations in the absence of the applied magnetic field for ultrathin ferromagnetic films with in-plane uniaxial and cubic anisotropies. One can easily find the analytic solutions of Eqs. (2) and (3) in the absence of the magnetic field, i.e., $H = 0$.

$\theta = 0^\circ, 90^\circ, 180^\circ, 270^\circ$

$$K_1 > 0 \text{ and } -K_1 < K_u < K_1, \tag{4a}$$

$\theta = 0^\circ, 180^\circ \quad K_u > 0$ and $-K_u \leqslant K_1 \leqslant K_u$, (4b)

$\theta = 90^\circ, 270^\circ \quad K_u < 0$ and $K_u \leqslant K_1 \leqslant -K_u$, (4c)

$\theta = \theta_0, -\theta_0, 180^\circ - \theta_0, 180^\circ + \theta_0$

$\theta_0 = \arcsin((K_1 + K_u)/2K_1)^{1/2}$

$$K_1 < 0 \text{ and } K_1 < K_u < -K_1. \tag{4d}$$

Fig. 2 gives the phase diagram of the spin configurations of the film system with zero applied field, where regions I–IV correspond to solutions (4a)–(4d), respectively. Under different conditions, three kinds of easy magnetization directions can be taken, namely, easy a-axis, easy b-axis and easy cone. Region I is divided into two subregions Ia and Ib, because the absolute energy minima among the four local energy minima in the two subregions differs from each other. Subregion Ib like region II takes easy a-axis, while subregion Ia like region III favors easy b-axis. It must be noted that the region III has a biaxial anisotropy and four local energy minima with spin orientations θ_0, $-\theta_0$, $180^\circ - \theta_0$, or $180^\circ + \theta_0$ have the same value of the energy. In this case the uniaxial anisotropy K_u only changes the value of the cone angle, does not affect the biaxial feature of the purely cubic anisotropy. The magnetization reversal processes in those regions would be discussed below.

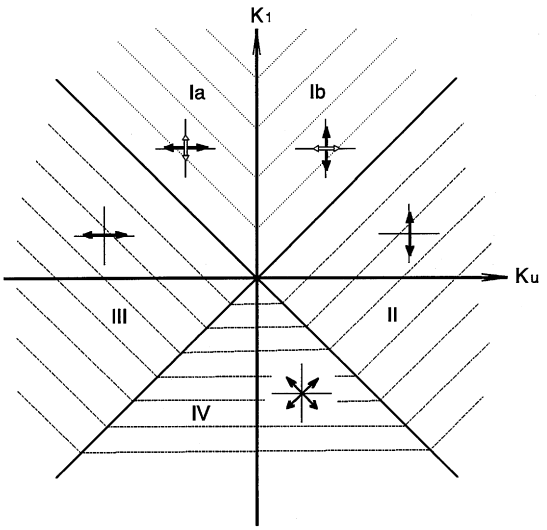

Fig. 2. Phase diagram of different spin configurations of an ultrathin ferromagnetic film with in-plane uniaxial and cubic anisotropies in the absence of an external magnetic field. The black arrows represent all possible directions of spin moment corresponding to the stablest energy minima. The blank arrows correspond to the metastable ones.

4. Magnetization reversal processes

In this section, magnetization reversal processes of the system studied will be discussed for three different cases in three subsections, respectively.

4.1. $K_1 > 0, -K_1 < K_u < K_1$

4.1.1. $|K_u| \ll K_1$

In regions Ia and Ib of Fig. 2 if $|K_u| \ll K_1$ and $H \ll K_1/M$, the solutions of Eqs. (2) and (3) will

always approximately be in the set $\{\theta = 0^\circ, \theta = 90^\circ, \theta = -90^\circ, \theta = -180^\circ\}$. These local energy minima can be found by substituting the relevant values of θ into Eq. (1):

$$E_{[1\ 0\ 0]} = -MH\cos\phi, \tag{5a}$$

$$E_{[-1\ 0\ 0]} = MH\cos\phi, \tag{5b}$$

$$E_{[0\ 1\ 0]} = K_u - MH\sin\phi, \tag{5c}$$

$$E_{[0-10]} = K_u + MH\sin\phi. \tag{5d}$$

The spin reversals between these four states will be mediated by the sweeping of 90° and 180° DWs. In Ref. [13] it was proved experimentally that $\varepsilon_{180^\circ} = 2\varepsilon_{90^\circ}$. When several possible jumps among these four states compete, we assume the one which can occur at the lower critical field is taken as the one observed actually. A magnetic phase diagram showing the number of irreversible jumps expected during the spin reversal was given by Cowburn et al. [14], only considering $K_u > 0$. In Fig. 3, we extend this phase diagram to the case of $K_u < 0$, and distinguish the region b from the region c, where their spin states are distinct. The spin states are shown schematically in the boxes. Two rows of boxes are displayed in each region. The lower one demonstrates the spin jumps on increasing the applied field, while the upper one corresponds to those when the applied field is decreased. It is worth noting that either 1-jump or 3-jump reversals experience the same routes on increasing and decreasing the external magnetic field, whereas 2-jump reversal undergoes different ones. The critical field of these spin jumps can be solved analytically by setting the energy advantage ΔE equal to the domain wall pinning energy ε between two spin stable states.

The hysteresis loops of the magnetization either parallel or perpendicular to the direction of the applied field, and the variation of the angle θ with respect to the applied field in different regions are shown in Fig. 4a. The magnetization reversal processes when $\varepsilon = 0$ are shown as dashed lines for comparison. Columns a–e correspond to the varied irreversible jumps in regions a–e in Fig. 3, respectively. These irreversible jumps on the hysteresis loops are markedly obvious. A very small uniaxial anisotropy can significantly influence the magnetization reversal process in a strong cubic anisotropy system. Changing the sign of K_u can also lead to a similar effect while only the spin states and the relation with respect to the applied field orientation are altered. This is because it does not matter for a cubic system where the uniaxial anisotropy is applied along the (1 0 0) or (0 1 0) axis. However, for the completeness of the phase diagram, we consider the case of $K_u < 0$ in Fig. 3. If $\varepsilon_{90^\circ} = 0$, i.e., $K_u/\varepsilon_{90^\circ} \to \infty$, one will see that only 1-jump or 3-jump reversals remain. No 2-jump reversal could be observed (no dashed lines in columns b–d of

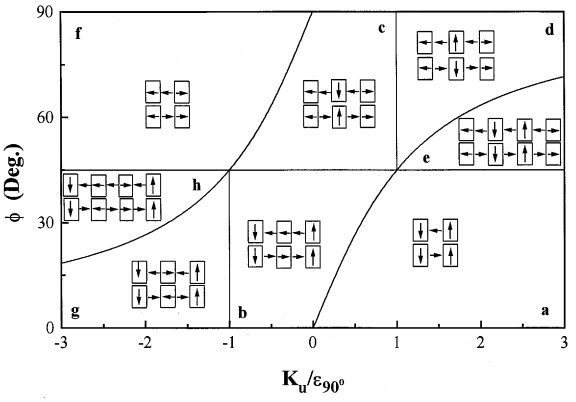

Fig. 3. Phase diagram of irreversible jumps expected during spin reversal as a function of the applied field orientation ϕ and the ratio of the in-plane uniaxial anisotropy K_u to the pinning energy ε_{90° of a 90° DW. The spin states on increasing and decreasing the field are shown schematically by the down and up rows of the boxes, respectively.

Fig. 4. (a) Hysteresis loops of the magnetization either parallel or perpendicular to the applied field and the variation of the spin states during the magnetization reversal processes. The parameters used during the calculation are: $K_u/M = 3$ Oe, $K_1/M = 275$ Oe, (a) $\phi = 35^\circ$, $\varepsilon_{90^\circ}/M = 3$ Oe; (b) $\phi = 35^\circ$, ε_{90°/M 5 Oe; (c) $\phi = 75^\circ$, $\varepsilon_{90^\circ}/M = 4$ Oe; (d) $\phi = 75^\circ$, $\varepsilon_{90^\circ}/M =$ 1.5 Oe; (e) $\phi = 75^\circ$, $\varepsilon_{90^\circ}/M = 0.5$ Oe. The dashed lines represent the magnetization reversal processes for $\varepsilon = 0$. (b) Hysteresis loops of the magnetization either parallel or perpendicular to the applied field and the variation of the spin states during the magnetization reversal processes. The parameters used during the calculation are: $K_u/M = 110$ Oe, $K_1/M = 275$ Oe, (a) $\phi = 35^\circ$, $\varepsilon_{180^\circ}/M = 150$ Oe; (c) $\phi = 80^\circ$, $\varepsilon_{180^\circ}/M = 250$ Oe; (d) $\phi = 80^\circ$, $\varepsilon_{180^\circ}/M = 100$ Oe; (e) $\phi = 80^\circ$, $\varepsilon_{180^\circ}/M = 20$ Oe. The dashed lines represent the magnetization reversal processes for $\varepsilon = 0$.

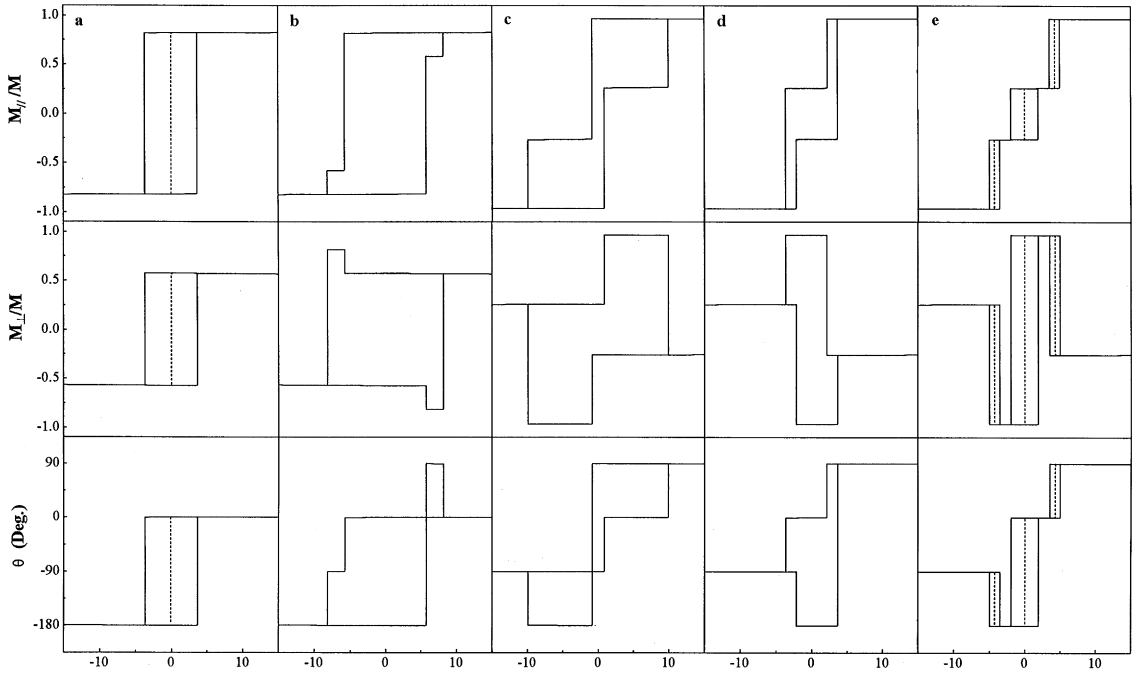

(a)

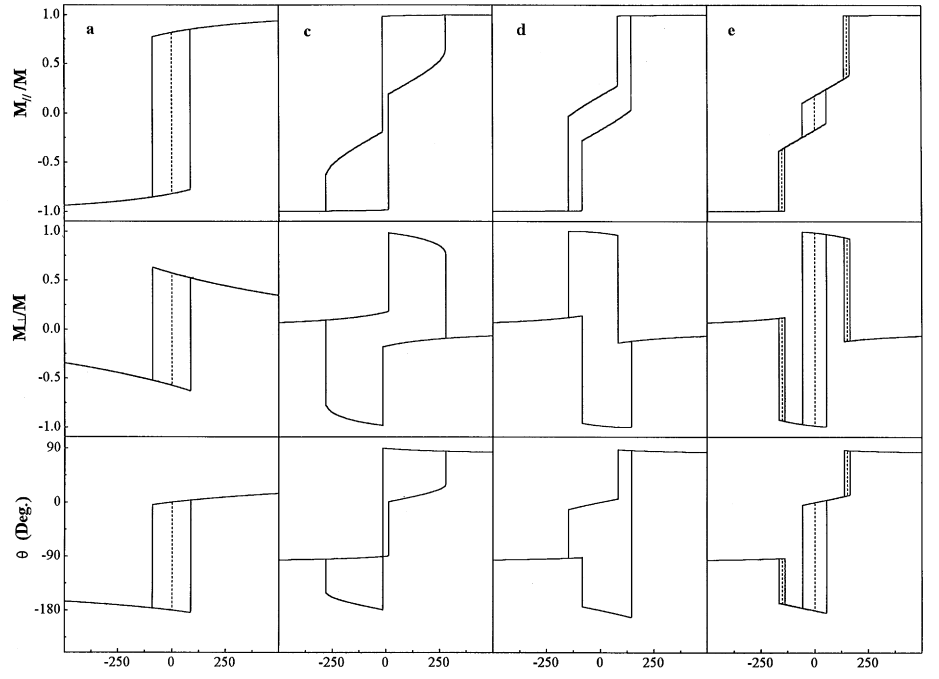

(b)

Fig. 4a) if only the absolute energy minimum were considered. Thus the occurrence of the 2-jump reversals must involve the mechanism of domain nucleation and propagation of the domain wall.

It is interesting to compare our numerical results with the hysteresis loops observed experimentally in literature. The hysteresis loops in columns a–c of Fig. 4a are similar to those denoted as I–III (and IV) in Fig. 3 of Ref. [13], observed in Ag/Fe/Ag(1 0 0). The hysteresis loops in column d seems to be of the same type as the Kerr signal in the right column of Fig. 13 of Ref. [23]. The hysteresis loop of 3-jumps in column e calculated for $\phi = 75^\circ$ is similar to that observed by Cowburn et al. [14] in a magnetic field at $\phi = 51^\circ \pm 3^\circ$. This is because we have given an example of 3-jumps for ϕ between 45° and 90°, where in a certain condition of $K_u/\varepsilon_{90^\circ}$ the hysteresis loops have the same characteristics.

4.1.2. $|K_u| \cong K_1$

If the strength of the uniaxial anisotropy is close to that of the cubic anisotropy, a low field would be insufficient to saturate the film. However, increasing the strength of the applied field will destroy the approximate analytic solutions of (2) and (3), and force the local energy minima away from the crystalline axes. In this case one has to develop a calculation procedure to determine the stable spin state at a certain magnetic field. Fig. 4b shows the calculation results for $K_u/K_1 = 0.4$. The dashed lines in columns a and e correspond to the results calculated by considering only the absolute energy minimum. It is similar to the case in Fig. 4a, but the first and third jumps of the 3-jump reversal in column e diverge from the crystalline axes. In this case if the propagation of the domain wall is taken into account the DW would no longer keep an angle of 90° or 180°. We assume that the pinning pressure of a θ DW is directly proportional to the value of its angle θ. During the numerical calculation, the phenomenological constant of a θ DW is defined as $\varepsilon_\theta = \varepsilon_{180^\circ} \cdot \theta/180$. Even if taking into account the propagation of the domain wall, one type of 2-jump reversal related to column b in Fig. 4a cannot be observed in Fig. 4b. This is due to the limitation of the DWs pinning energy, beyond which the coherent rotation would dominate the magnetization reversal process. A coherent rotation model is requested to describe such a process in this case. The hysteresis loops possessing the same shape as in columns (a) and (c) in Fig. 4b have been frequently observed in Fe/GaAs(0 0 1) [5,10,12].

4.2. $|K_u| > |K_1|$

Now, let us consider what will happen if $K_u > K_1$ as in the region II of Fig. 2. As the strength of the uniaxial anisotropy is stronger than that of the cubic anisotropy, only two local energy minima appear at zero applied field since the other two are eliminated. At low field there is nothing but a 1-jump reversal mediated by the sweeping of the 180° DW, irrespective of the direction of the applied field. We need to increase the strength of the applied field in order to detect more jumps. Fig. 5 displays the simulation results for $K_u/K_1 = 1.1$. The shape of the hysteresis loops resembles that in Fig. 4b. But one type of 2-jump reversal related to column c in Fig. 4b vanishes in Fig. 5. The reason is the same as the above mentioned (in Section 4.1.2). Further increasing the strength of the uniaxial anisotropy, the critical fields for the first and third jumps in the case of 3-jump reversal will be gradually enhanced and finally the jumps disappear at a certain point, where the 3-jump reversal turns into a 1-jump one. What happens in region III in Fig. 2 is analogous to that in region II. Therefore, the influence of an in-plane uniaxial anisotropy on the jumps in the magnetization reversal processes of an ultrathin cubic ferromagnetic film would be weakened, and the critical fields would be greatly enhanced by increasing the strength of the uniaxial anisotropy.

4.3. $K_1 < 0, K_1 < K_u < -K_1$

In this case, in the absence of the external magnetic field, the easy magnetization direction deviates from the crystallographic directions. The simulation results are different from those in other regions. No more jumps occur in the magnetization curves except for 2-jump spin reversal, as shown in Fig. 6. The dashed lines also prove that in the case of considering the absolute energy minima, only

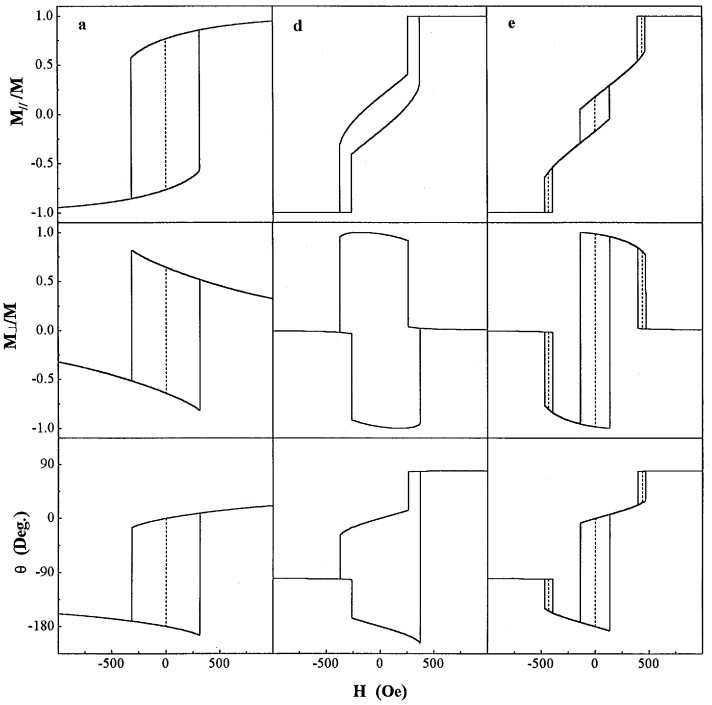

Fig. 5. Hysteresis loops of the magnetization either parallel or perpendicular to the applied field and the variation of the spin states during the magnetization reversal processes. The parameters used during the calculation are: $K_u/M = 300$ Oe, $K_1/M = 275$ Oe, (a) $\phi = 40^\circ$, $\varepsilon_{180^\circ}/M = 500$ Oe; (d) $\phi = 80^\circ$, $\varepsilon_{180^\circ}/M = 200$ Oe; (e) $\phi = 80^\circ$, $\varepsilon_{180^\circ}/M = 50$ Oe. The dashed lines represent the magnetization reversal processes for $\varepsilon = 0$.

1-jump reversal can take place no matter what direction the magnetic field is applied. For $K_u \ll |K_1|$ and $K_u = -K_1/2$, one obtains the cone angles $\theta_0 = 45^\circ$ and 30°, respectively. When a low field is applied, four states with spin orientations θ_0, $-\theta_0$, $180^\circ - \theta_0$, $180^\circ + \theta_0$ are the stable states. If the energy advantages between these states satisfy the density cost in unpinning a DW of one of the three types, $\varepsilon_{2\theta}$, $\varepsilon_{180^\circ-2\theta}$ and ε_{180° which are directly proportional to the angle of the DW, the spin orientation will rotate from one state to another stabler one. It can be seen, from the four columns in Fig. 6 that only 2-jump spin reversal occurs between these four states, regardless of the values of the cone angle θ_0, the applied field orientation ϕ and the ratio of $K_u/\varepsilon_{180^\circ}$. They are similar to the case of $K_u = 0$ in Fig. 3 when no uniaxial anisotropy is taken into account. This behavior can be attributed to the unique biaxial anisotropy of this system at zero applied field. This kind of 2-jump spin reversal processes was found experimentally by Diao et al. in Co/Cu/Co sandwich structures [17].

5. Discussions and conclusion

In this work, based on the consideration of the domain process, we attain a clear cognizance of the spin reversals in ultrathin ferromagnetic films with in-plane uniaxial and cubic anisotropies. These results have certain significance in both theoretical and experimental aspects. They provide a criterion of the possible mechanism of spin reversal in ultrathin films, which is closely related with the spin configurations in the absence of the magnetic field.

Recent advances in thin-film growth techniques have enabled us to establish new phases of magnetic materials. Cobalt, which naturally occurs in the hexagonal close-pack phase, has been grown in

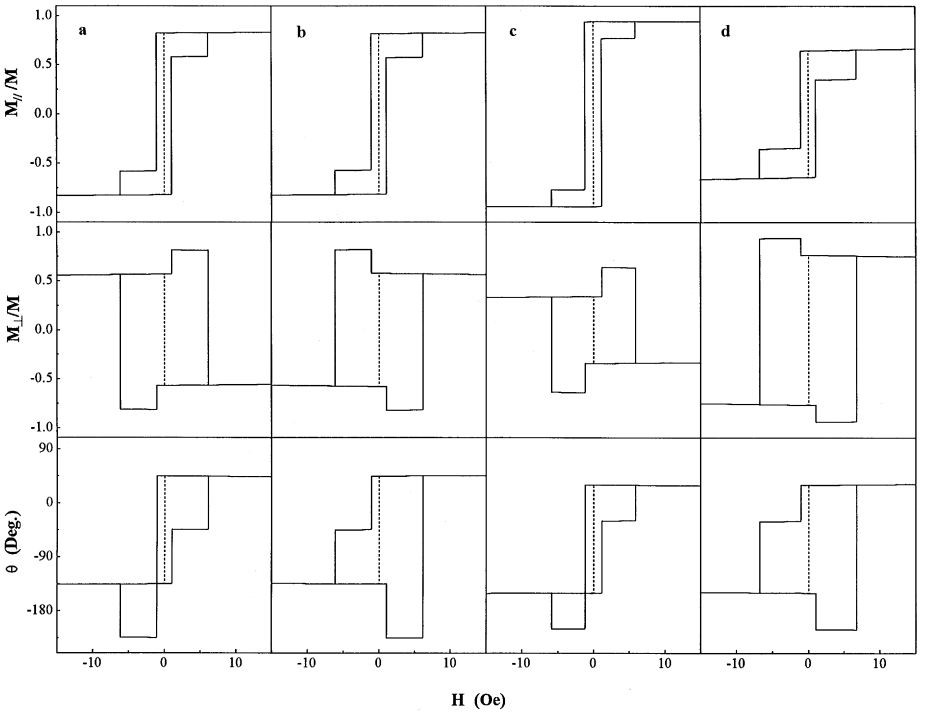

Fig. 6. Hysteresis loops of the magnetization either parallel or perpendicular to the applied field and the variation of the spin states during the magnetization reversal processes. The parameters used during the calculation are: (a) $K_u/M = 3$ Oe, $K_1/M = -275$ Oe, $\phi = 10^\circ$, $\varepsilon_{90^\circ}/M = 1$ Oe; (b) $K_u/M = 3$ Oe, $K_1/M = -275$ Oe, $\phi = 80^\circ$, $\varepsilon_{90^\circ}/M = 1$ Oe; (c) $K_u/M = 137.5$ Oe, $K_1/M = -275$ Oe, $\phi = 10^\circ$, $\varepsilon_{180^\circ}/M = 3$ Oe; (d) $K_u/M = 137.5$ Oe, $K_1/M = -275$ Oe, $\phi = 80^\circ$, $\varepsilon_{180^\circ}/M = 3$ Oe. The dashed lines represent the magnetization reversal processes for $\varepsilon = 0$.

metastable FCC and BCC phases as thin supported films. Generally, these ultrathin Co films have the easy magnetization direction along the $\langle 1\,1\,0\rangle$ axis, indicating that $K_1 < 0$ [15–18,24–26]. On the other hand, the easy magnetization direction of the Fe films is usually along the $\langle 1\,0\,0\rangle$ axis, i.e., $K_1 > 0$ [10–14]. It is a common phenomenon in ultrathin cubic ferromagnetic films that an additional in-plane uniaxial anisotropy is introduced. It can be attributed to several mechanisms, for example, the oblique incidence of deposition particles [27,28], lattice mismatch strain-induced magnetoelastic effects [29,30], atomic steps on the interface [31–36], the internal oxidation along the oxygen chains on the surface of the substrate (Al_2O_3, MgO) [36,37], or dangling bands on the arsenic/gallium rich surface [12]. Moreover, the strength of the uniaxial anisotropy is dependent on the thickness of the film [2,23]. One can obtain cubic ferromagnetic films with different values of K_1 and K_u after accurately controlling the composition and the microstructure of the film and substrate. According to the consequence of this work, one can take a prior prediction of the pattern of the spin reversal in the films.

In conclusion, we have investigated the influence of an in-plane uniaxial anisotropy on the magnetization reversal processes of ultrathin cubic ferromagnetic films. The phase diagram of the spin configurations of this system in the absence of the applied field has been derived. The spin reversals induced by the applied field via the absolute energy minimum or the propagation of the DW have been studied numerically. Increasing the strength of the uniaxial anisotropy diminishes its effect on jumps in the magnetization reversal processes. If a cone

angles present in the absence of the magnetic field, the uniaxial anisotropy does not change the biaxial anisotropy of this cubic system, but the value of the cone angle, and no more jumps can take place.

Acknowledgements

This work has been supported by the project No. 59725103 of the National Sciences Foundation of China and by the Science and Technology Commission of Shenyang and Liaoning.

References

[1] N.D. Mermin, H. Wagner, Phys. Rev. Lett. 17 (1966) 1133.
[2] M.T. Johnson, P.J.H. Bloemen, F.J.A. den Broeder, J.J. de Vries, Rep. Prog. Phys. 59 (1996) 1409.
[3] J.A.C. Bland, R.D. Bateson, P.C. Riedi, R.G. Graham, H.J. Lauter, J. Penfold, C. Shackleton, J. Appl. Phys. 69 (1991) 4989.
[4] E. Gu, J.A.C. Bland, C. Daboo, M. Gester, L.M. Brown, R. Ploessl, J.N. Chapman, Phys. Rev. B 51 (1995) 3596.
[5] C. Daboo, R.J. Hicken, E. Gu, M. Gester, S.J. Gray, D.E.P. Eley, E. Ahmad, J.A.C. Bland, R. Ploessl, J.N. Chapman, Phys. Rev. B 51 (1995) 15964.
[6] M. Gester, C. Daboo, R.J. Hicken, S.J. Gray, A. Ercole, J.A.C. Bland, J. Appl. Phys. 80 (1996) 347.
[7] G.W. Anderson, P. Ma, P.R. Norton, J. Appl. Phys. 79 (1996) 5641.
[8] E.M. Kneedler, B.T. Jonker, P.M. Thibado, R.J. Wagner, B.V. Shanabrook, L.J. Whiteman, Phys. Rev. B 56 (1997) 8163.
[9] K. Postava, H. Jaffres, A. Schuhl, F. Nguyen Van Dau, M. Goiran, A.R. Fert, J. Magn. Magn. Mater. 172 (1997) 199.
[10] J.M. Florczak, E. Dan Dahlberg, Phys. Rev. B 44 (1991) 9338.
[11] J.R. Childress, R. Kergoat, O. Durand, J.M. George, P. Galtier, J. Miltat, A. Schuhl, J. Magn. Magn. Mater. 130 (1994) 13.
[12] C. Daboo, R.J. Hicken, D.E.P. Eley, M. Gester, S.J. Gray, A.J.R. Ives, J.A.C. Bland, J. Appl. Phys. 75 (1994) 5586.
[13] R.P. Cowburn, S.J. Gray, J. Ferré, J.A.C. Bland, J. Miltat, J. Appl. Phys. 78 (1995) 7210.
[14] R.P. Cowburn, S.J. Gray, J.A.C. Bland, Phys. Rev. Lett. 79 (1997) 4018.
[15] A. Cebollada, J.L. Martínez, J.M. Gallego, J.J. de Miguel, R. Miranda, S. Ferrer, F. Batallán, G. Fillion, J.P. Rebouillat, Phys. Rev. B 39 (1989) 9726.
[16] G.R. Harp, S.S.P. Parkin, Appl. Phys. Lett. 65 (1994) 3063.
[17] Z.T. Diao, S. Tsunashima, M. Jimbo, S. Iwata, J. Phys.: Condens. Matter. 8 (1996) 4959.
[18] Z.Q. Qiu, J. Pearson, S.D. Bader, J. Appl. Phys. 73 (1993) 5765.
[19] E.C. Stoner, E.P. Wohlfarth, Philos. Trans. R. Soc. London A 240 (1948) 74.
[20] B. Dieny, J.P. Gavigan, J. Phys.: Condens. Matter. 2 (1990) 187.
[21] J.L. Robins, R.J. Celotta, J. Unguris, D.T. Pierce, B.T. Jonker, G.A. Prinz, Appl. Phys. Lett. 52 (1988) 1918.
[22] J. Pommier, P. Meyer, G. Pénissard, J. Ferré, P. Bruno, D. Renard, Phys. Rev. Lett. 65 (1990) 2054.
[23] R.P. Cowburn, J. Ferré, J.P. Jamet, S.J. Gray, J.A.C. Bland, Phys. Rev. B 55 (1997) 11593.
[24] C.H. Lee, H. He, F. Lamelas, Phys. Rev. B 62 (1989) 653.
[25] F.J. Lamelas, C.H. Lee, H. He, W. Vavra, R. Clarke, Phys. Rev. B 40 (1989) 5837.
[26] G.A. Prinz, Phys. Rev. Lett. 54 (1985) 1051.
[27] O. Durand, J.R. Childress, P. Galiter, R. Bisaro, A. Schuhl, J. Magn. Magn. Mater. 145 (1995) 111.
[28] Y. Hoshi, E. Suzuki, M. Naoe, J. Appl. Phys. 79 (1996) 4945.
[29] S. Subramanian, X. Liu, R.L. Stamps, R. Sooryakumar, G.A. Prinz, Phys. Rev. B 52 (1995) 10194.
[30] A. Berger, U. Linke, H.P. Oepen, Phys. Rev. Lett. 68 (1992) 839.
[31] J. Chen, J.L. Erskine, Phys. Rev. Lett. 68 (1992) 1212.
[32] H.P. Oepen, A. Berger, C.M. Schneider, T. Reul, J. Kirschner, J. Magn. Magn. Mater. 121 (1993) 490.
[33] P. Krams, B. Hillebrands, G. Güntherdot, H.P. Oepen, Phys. Rev. B 49 (1994) 3633.
[34] W. Wulfhekel, S. Knappman, H.P. Oepen, J. Appl. Phys. 79 (1996) 988.
[35] R.K. Kawakami, Ernesto J. Escorcia-Aparico, Z.Q. Qiu, Phys. Rev. Lett. 77 (1996) 2570.
[36] N. Metoki, M. Hofelich, Th. Zeidler, Th. Mühge, Ch. Morawe, H. Zabel, J. Magn. Magn. Mater. 121 (1993) 137.
[37] Yu.V. Goryunov, G.G. Khaliulin, I.A. Garifullin, L.R. Tagirov, F. Schreiber, P. Bödeker, K. Bröhl, Ch. Morawe, Th. Mühge, H. Zabel, J. Appl. Phys. 76 (1994) 6096.